Conf-920792--15

Coherent Nuclear Resonant Optics for Third Generation Synchrotron Radiation Sources*

E.E. Alp, T. M. Mooney and T. Toellner
Advanced Photon Source
Argonne National Laboratory
9700 South Cass Avenue
Argonne, IL 60439

and

H. Homma and M. Kentjana
Brooklyn College
CUNY
Brooklyn, NY 11210

June, 1992

ANL/CP--76527

DE92 017095

cz

*This work supported by the U.S. Department of Energy, BES-Materials Sciences, under contract no. W-31-109-ENG-38

COHERENT NUCLEAR RESONANT OPTICS FOR THIRD GENERATION SYNCHROTRON RADIATION SOURCES (*)

E. E. Alp, T. M. Mooney, T. Toellner

Advanced Photon Source, Argonne National Laboratory
Argonne, Illinois 60439

and

H. Homma, M. Kentjana
Brooklyn College, CUNY, Brooklyn, NY 11210

ABSTRACT

The insertion-device-based, third-generation, synchrotron radiation sources now under construction in Europe, the USA, and Japan bring new opportunities and challenges in the design and manufacture of x-ray optics. These high brightness sources provide new opportunities to overcome some of the outstanding problems associated with nuclear resonant monochromatization of synchrotron radiation. New methods such as polarizing monochromators, and zone plates provide alternative methods for production of μeV-neV resolution in the hard x-ray regime. The design principles, and characterization, and performance of crystal monochromators and of nuclear coherent scattering optics, including Grazing Incidence Anti Reflection (GIAR) films, multilayers, zone plates, as well as single crystals are discussed.

INTRODUCTION

New x-ray optics components are being developed to obtain μeV-neV energy resolution for hard x-rays generated by insertion-device-based, third generation, synchrotron radiation sources. At present, there are three projects under construction: the European Synchrotron Radiation Facility (ESRF) in Grenoble, France, the Advanced Photon Source (APS) in Argonne National Laboratory, USA, and the 8 GeV project (SPring-8) in Harima Science Garden City, Japan. The expected completion dates are 1993, 1996, and 1998, respectively. The unique and common feature of all these new sources is the combination of low-particle-beam emittance in the storage ring, low x-ray beam divergence, and high x-ray beam intensity generated by undulators and wigglers.

The monochromatization of x-rays to the μeV-neV level is achieved by nuclear resonant scattering [1-5]. The energy bandpass achievable is directly proportional to the lifetime of the excited states of the Mossbauer nuclei. The current challenge is to design and

---

(*) Work supported by US-DOE, BES Materials Science, under contract No: W-31-109-ENG-38.

develop new optics and experimental techniques to tailor the energy, time, polarization, and focussing response of the optical components to experimental needs. We group these activities into the following categories:

1. Crystal monochromators
2. Nuclear monochromators
3. Focusing devices
4. Alternative methods

In the following, we will address the issues relevant to each of the above. The goal is to first produce a beam of unprecedented energy resolution and intensity and to develop experiments that will take advantage of this unusual beam. The examples discussed are based on three different Mossbauer isotopes: ^{169}Tm at 8410 eV, ^{57}Fe at 14413 eV, and ^{119}Sn at 23870 eV.

1. CRYSTAL MONOCHROMATORS

The monochromatization of x-rays is typically achieved by diffraction from nearly perfect crystals. The degree of monochromatization is given by :

$$\left(\frac{\Delta E}{E}\right)^2 = \left(\frac{\Delta d}{d}\right)^2 + (\Delta\theta_s \cot\theta)^2 ,$$

where the first term describes the crystal perfection, and the second term is a manifestation of the finite extinction length. The high-energy-resolution crystal monochromators commonly in use today are generally limited by extinction length rather than by crystal imperfection. In this case, the energy resolution achievable by Bragg diffraction from thick perfect crystals is limited by the Bragg angle and the angular acceptance according to the relationship $\Delta E = E.\cot\theta\,\Delta\theta$. The Darwin width, $\Delta\theta = \frac{1}{\sqrt{b}}\frac{2}{\sin 2\theta}\frac{r_e\lambda^2}{\pi V}C|F_H|e^{-M}$, where r_e = classical electron radius, λ = wavelength, and $b = \frac{\sin(\theta-\alpha)}{\sin(\theta+\alpha)}$ is the asymmetry parameter, α is angle between Bragg planes and the crystal surface, θ is the Bragg angle, V is the unit cell volume, C is the polarization factor ($\cos 2\theta$ for π-polarized radiation or C = 1 for σ-polarized radiation), $|F_H|$ is the structure factor in the scattering direction, and e^{-M} is the Debye-Waller factor[6]. The expected energy resolution and angular acceptance for several Bragg reflections for Si monochromators are tabulated in Table 1 for 8410, 14413, and 23870 eV radiation corresponding to ^{169}Tm, ^{57}Fe, and ^{119}Sn resonances, respectively. Compared to the angular divergence of the undulator ($\approx$ 5 arcsec) none of the high order reflections are efficient monochromators.

Table 1. The calculated angular acceptance and energy resolution of various reflections at ^{169}Tm , ^{57}Fe , and ^{119}Sn Mossbauer resonance energies.

Isotope	^{169}Tm			^{57}Fe			^{119}Sn		
Energy(eV)	8410			14413			23870		
Reflection	θ (deg)	Δθ (sec)	ΔE (eV)	θ (deg)	Δθ (sec)	ΔE (eV)	θ (deg)	Δθ (sec)	ΔE (eV)
1 1 1	14.3	6.9	1.05	7.88	3.75	1.89	4.75	2.24	3.13
2 2 0	22.57	4.87	0.48	12.94	2.7	0.82	7.77	1.60	1.36
4 2 2	41.68	2.57	0.12	22.83	1.21	0.2	13.55	0.70	0.34
3 3 3	44.85	1.72	0.07	24.30	0.78	0.12	14.39	0.44	0.20
5 5 5				43.30	0.30	0.02	24.46	0.15	0.04
8 4 0				45.1	0.41	0.03	25.32	0.19	0.05
10 6 4				77.5	0.50	0.008	36.13	0.08	0.01

High Energy Resolution, Large Angular Acceptance Crystal Monochromator

The monochromatization of white x-ray spectrum to the μev-neV level is a difficult exercise in improving signal-to-background ratio. The radiation generated by an undulator is considered pseudo-monochromatic, in the sense that there is an increased intensity of about 10^1-10^3 orders of magnitude around the first and few harmonics. The spectral distribution of a typical undulator on the APS ring is given in Fig. 1. The width of the first harmonic at 14.4 keV is around 2.5 keV for this device. A Si (111) double crystal monochromator placed on the beamline will cut this width down to few eV, and will handle the high power density generated by the undulator source. The energy width can be further improved to a level of 5-50 meV by adding a second crystal monochromator involving higher order reflections [7]. However, the angular acceptance of higher order reflections is narrower than one arcsec, and a significant penalty in terms photon flux is accepted in this method of monochromatization.

An alternative method, that combines asymmetrically cut crystals to reduce the beam divergence with high order reflections to obtain high energy resolution has been suggested[8]. In this method, the angular divergence of the incident x-ray beam is reduced by diffracting from an asymmetrically cut crystal. This beam is further diffracted by a high- order reflection monochromator to improve the energy resolution, but without much loss due to low angular acceptance, finally the original beam can be recovered by a crystal of the same cut as the first one, but with a different sign of asymmetry angle. The energy bandpass achievable with such monochromators are 10 meV at 14413 eV ($\Delta E/E = 7 \times 10^{-7}$) for the ^{57}Fe resonance and 40 meV at 23870 eV ($\Delta E/E = 1.5 \times 10^{-6}$) for the ^{119}Sn nuclear resonance with angular acceptance of 4" and 2", respectively. The details of construction and testing of these monochromators are described by Toellner, et al (9) in these proceedings.

Polarizing Monochromator

The polarization dependence of the angular acceptance of perfect crystals is described by , $C = \cos 2\theta$ for π-polarized radiation. In σ (π) polarization the electric field vector is perpendicular (parallel) to the scattering plane defined by incident and scattered beam. For a Bragg angle near 45°, the π component will have an angular acceptance close to zero. This is used to design polarizers in the hard x-ray regime.[10-11] For example, Si (333), Si (840) and Si (12 6 6) each provides a near 45° Bragg angle for the ^{169}Tm, ^{57}Fe, and ^{119}Sn isotopes, respectively. The proposed experimental set-up is shown in Fig. 2. A channel-cut monochromator (P) polarizes the incident beam to 1 part in 10^4-10^7, and thus an analyzer crystal (A) of the same reflection placed perpendicularly to the first one will suppress the σ-polarized beam at the same level. If a σ to π scattering process takes place in between the polarizer and analyzer, then the π component will pass through the analyzer.

Nuclear transitions allowed by magnetic dipole selection rules cause strong σ to π resonant scattering, and this can be filtered at the expense of the non-resonant part, eliminating the overwhelming initial flux. However, scattering in the horizontal plane is not desirable for a bending magnet or a wiggler source with a horizontal divergence of few milliradians, and it costs more than a factor of 3 orders of magnitude in flux. On the other hand, with an undulator source, the vertical and horizontal angular divergences are about 5 and 10 arcsec, respectively.[12] Furthermore, the angular acceptance can be increased by asymmetrically cutting the channel-cut crystals. The results of such an exercise are given in Table 2, and the reflectivities are shown in Fig. 3. The conclusion is that one can provide a polarizing monochromator with a non-resonant background rejection ratio of 10^{-8}, and still obtain reasonable flux at the detector with undulator sources. However, the angular acceptance at very high energies like that of ^{119}Sn at 23870 eV are still very narrow and some other alternative is desirable.

Table 2. The calculated angular acceptance and the degree of linear polarization attainable for ^{169}Tm, ^{57}Fe, and ^{119}Sn Mossbauer resonance energies.

Isotope		^{169}Tm			^{57}Fe			^{119}Sn	
Energy(eV)		8410			14413			23870	
Reflection		Si (3 3 3)			Si (8 4 0)			Si (12 6 6)	
Bragg angle(degrees)		44.7			45.1			44.65	
α	1/b	$\Delta\theta$ (sec)	S* (10^{-7})	1/b	$\Delta\theta$ (sec)	S* (10^{-7})	1/b	$\Delta\theta$ (sec)	S* (10^{-7})
0	1	1.72	1.1	1	0.37	6.19	1	0.04	1900
-40	12.1	5.5	0.28	11.2	1.24	0.33	12.2	0.13	42
-43	33.6	9.5	0.10	27.2	1.94	0.12	34.7	0.23	0.07

(*)S is the square of the ratio of the area under the π-reflectivity curve to that of σ-reflectivity curve, indicating the degree of possible linear polarization using a channel-cut crystal with two bounces.

2. NUCLEAR MONOCHROMATORS

The last step of monochromatization is based on the narrow energy linewidth of Mossbauer nuclear resonance. Under suitable conditions, the reflectivity of such media can be enhanced for nuclear resonant photons only at the expense of photons outside the resonance linewidths, hence further monochromatization can be achieved either by reflection,[13] diffraction,[14] or focussing.[15] Such media include single crystals and artifically synthesized multilayers, where reflectivity is based on whether the incident photon is resonant with the medium or not. For example, a single crystal of Yttrium Iron Garnet (YIG),[1,3] Fe_2O_3,[2] $FeBO_3$,[5] or Thullium Iron Garnet (TIG)[16] can be oriented so that the electronic reflection is forbidden, while the nuclear reflection is allowed. Such crystals have been used so far very successfully. However, these crystals are hard to grow, limited in number. In addition, the nuclear levels are split by internal hyperfine fields, resulting in a beam that has time beats complicating the data analysis. It would be desirable to develop newer optics to perform a similar role and which can be synthesized easily. GIAR films and multilayers, in this sense, are very promising. A medium containing periodic and alternating layers of resonant and nonresonant material will reflect or diffract the resonant radiation with some efficiency.

Grazing Incidence Anti Reflection (GIAR) Films:

The sharp contrast between the electronic and nuclear indices of refraction allows to design monochromators in which the electronic reflectivity is sharply reduced at a specific angle, while the nuclear reflectivity is still substantial. Such materials have been proposed,[17] synthesized,[18] and tested.[19] The large difference in electronic and nuclear absorption cross sections (more than two orders of magnitude) provide an opportunity to design the thickness of the thin film layers so that x-rays reflected from electron charge interfere destructively at a given angle, and there is still appreciable reflectivity for x-rays resonantly scattered by nuclei.

The performance of GIAR films depends critically on the following factors: i) degree of suppression and absolute nuclear reflectivity, ii) energy bandpass and nuclear decay rate, and iii) surface roughness and incident beam angular divergence. The degree of suppression can be defined as the ratio of resonant nuclear reflectivity to that of non-resonant electronic reflectivity at a given angle. This is shown in Fig 4 (a)-(d) for the system SnO_2/Pd which has been described previously,[20,21] as well as in these proceedings.[22] Realistically, one should expect a suppression of 10 to 50 for "damping stabilized" films in which the operating point is at a lower angle, around 2 mrad. The energy bandpass in this case is relatively large, $\pm$ 100 Γ, corresponding to an energy resolution of 2.5 μeV. However, this broadening in energy corresponds to a faster decay rate, and time filtering using the coincidence techniques becomes difficult. The use of either a high-energy resolution monochromator or a polarizing monochromator in connection with faster detectors may help for high-energy transitions. Also, the suppression level is strongly dependent on the incident beam divergence, and this should be kept under 2 arcsec.

It is clear that these monochromators are capable of producing μeV resolution, which may prove to be very useful in inelastic scattering studies.

Multilayer Structures

An alternative to perfect crystals with electronically forbidden, nuclear-allowed reflection is the idea of multilayers alternately containing nuclear resonant/nonresonant atoms. This arrangement periodically varies the index of refraction for nuclear resonant radiation with a uniform index of refraction for nonresonant part of the radiation. (23,24) The Bragg angle can be adjusted by adjusting the layer thickness. The limiting factor is the interface roughness, which needs to be minimized with respect to layer thickness. The expected performance of a 20 Å - 50 layer $^{119}SnO_2$ - $^{120}SnO_2$ system is calculated in Fig. 5 (a)-(d), assuming an interface roughness of 5 Å. The Bragg peak at 6.9 mrad indicates the measure of suppression obtainable, which is better than two orders of magnitude. As expected, the position of the Bragg peak is a strong function of the deviation from nuclear resonant energy. One consequence of higher incident angles is the narrower energy width compared to the GIAR case. In addition, the operating angle is adjustable by changing the periodicity of the layers. The advantage of multilayers over GIAR films is the elimination of the need for long films due to higher operating angles.

3. FOCUSING OPTICS : Mossbauer-Fresnel Zone Plates

The size of the undulator beam varies for each facility but is expected to be around 1.5 mm in the vertical and 3 mm in the horizontal direction, at a distance of 70 m from the source point. It has been proposed that a Fresnel zone plate consisting of alternating zones of resonant - nonresonant medium will focus the resonant portion of the incident x-ray beam to few μm spot size, thus providing the needed monochromatization and spatial focusing.(15) The operating principle here is again the large difference in the index of refraction between nuclear resonant, and nonresonant radiation. The zone plate will focus only the nuclear resonant portion of the radiation and,with a aid of a pinhole, this can be filtered. The calculated performance of this device for ^{57}Fe in a non-magnetic environment is shown in Fig. 6. The focusing efficiency and the energy bandpass depend on the zone plate thickness. The monochromatization efficiency, however, depends on the number of zones available and the focal spot size, both of which are limited by the microfabrication techniques. With the current state-of-the-art technology, it may be possible to produce a zone plate with 0.2 μm final zone thickness. Then, for a focal length of 2 m, a zone-plate diameter of 0.86 mm, and a focal spot size of 3 μm, a monochromatization efficiency of 10^5 is expected. Of course, a focusing device of this nature would also useful for studying small samples and for high-pressure experiments.

4. ALTERNATIVE METHODS

The 3rd generation synchrotron sources also provide intense x-rays above 100 keV. The monochromatization of x-rays in this energy regime is accomplished by using curved crystals in the Laue geometry.(25) Then, it is, in principle possible to excite higher nuclear

energy levels, and discriminate against the prompt peak by energy discrimination using a pulse height analyzer. This is a promising method if the purpose is to observe the Mossbauer effect on a difficult isotope. However, the re-emitted radiation is no longer coherent in a given direction, and therefore, this method of monochromatization does not preserve the high brightness of the incident beam.

5. CONCLUSIONS

A review has been presented discussing some of the current nuclear resonant x-ray optic development efforts taking place in preparation of the dedicated beamlines at the third generation synchrotron radiation sources. The unprecedented brightness of the undulator sources enables novel optics development that were unthinkable a decade ago.

ACKNOWLEDGMENTS

We would like to acknowledge many useful discussions with D. M. Mills, A. M. Macrander, W. Yun, D. Haeffner and G. Srajer of Argonne National Laboartory, and E. Gerdau, and W. Sturhahn and E. Witthoff of Hamburg University, and S. Ruby and J. Arthur of SSRL.

REFERENCES

1. E. Gerdau, R. Rüffer, H. Winkler, W. Tolksdorf, C. P. Klages, and J. P. Hannon, Phys. Rev. Lett. **54**, 835 (1985).
2. G. Faigel, D. P. Siddons, J. B. Hastings, P. E. Haustein, J. R. Grover, and L. E. Berman, Phys. Rev. Lett. **61**, 2794 (1988).
3. J. Arthur, G. S. Brown, D. E. Brown, and S. L. Ruby, Phys. Rev. Lett. **63** ,1629 (1989).
4. S. Kikuta, Y. Yoda, Y. Hasegawa, K. Izumi, T. Ishikawa, X. W. Zhang, S. Kishimoto, H. Sugiyama, T. Matsushita, M. Ando, C. K. Suzuki, M. Seto, H. Ohno, H. Takei, ICAME91, Hyperfine Interactions (1992).
5. A. I. Chumakov, M. V. Zelepukhin, G. V. Smirnov, U. van Bürck, R. Rüffer, R. Hollatz, H. D. Rüter, and E. Gerdau, Phys. Rev. B. **41** 9545 (1990).
6. T. Matsushita, H. Hashizume, **Handbook on Synchrotron Radiation**, vol 1. Ed. E. E. Koch, North-Holland Pub. Co., p. 161 (1983).
7. D.P. Siddons, J.P. Hastings, G. Faigel, J. R. Grover, P. E Haustein, L. E. Berman, Rev. Sci. Instrum. **60**,1649 (1989).
8. T. Ishikawa, Y. Yoda, K. Izumi, C. K. Suzuki, X. W. Zhang, M. Ando, S. Kikuta, Rev, Sci, Instr. **63**, 1015 (1992).
9. T. Toellner, T. Mooney, S. Shastri, E. E. Alp, SPIE (1992) proceedings
10. M. Hart, A. R. D. Rodrigues, Philos.Mag. B **40**, 149 (1979).
11. D. P. Siddons, M. Hart, Y. Amemiya, J. B. Hastings, Phys. Rev. Lett. **64** 1967 (1990).
12. G. Shenoy, J. P. Viccaro, D. M. Mills, ANL-88-9, Argonne, (1988).
13. J. P. Hannon, G. T. Trammel, M. Mueller, E. Gerdau, H. Winkler, and R. Rüffer, Phys. Rev. Lett. **43**, 636(1979).
14. S. Ruby, J. Phys. (Paris), Colloq. 35, C6-209 (1974).
15. T. Mooney, W. Yun, E. E. Alp, J. Appl. Phys, June 1992 (in print).
16. W. Sturhahn, E. Gerdau, R. Hollatz, R. Ruffer, H. D. Ruter, W. Tolksdorf, Europhys. Lett. **14** 821 (1991).

17. J. P. Hannon, N. V. Hung, G. T. Trammel, E. Gerdau, M. Mueller,R. Rüffer, and H. Winkler, Phys. Rev. B. **32** 5068 (1985) , Phys. Rev. B. **32** 5081 (1985) ,Phys. Rev. B. **32** 6363 (1985) , Phys. Rev. B. **32** 6374 (1985) .
18. M. Grote, R. Rohlsberger, E. Gerdau, R. Helmmich, M. Harsdorff, M. Chambers, W. Pfutzner, Hyperfine Interactions **58**, 2439 (1989).
19. M. Grote, R. Rohlsberger, M. Dimer, E. Gerdau, R. Helmmich, R. Hollatz, J. Jaschke, E. Luken, J. Metge, R. Ruffer, H. D. Ruter, W. Sturhahn, E. Witthoff, M. Harsdorff, W. Pfutzner, M. Chambers, J. P. Hannon, Euro. Phys. Lett. **17** 707 (1991).
20. M. Kentjana, H. Homma, E. E. Alp, T. M. Mooney, SPIE proceedings **1546** (1991).
21. H. Homma, M. Kentjana, E. E. Alp, T. M. Mooney, E. Witthoff, T. Toellner, J. Appl. Phys. (in print)
22. H. Homma, M. Kentjana, E. E. Alp, T. M. Mooney, E. Witthoff, T. Toellner,SPIE (1992) proceedings.
23. A. I. Chumakov, G. V. Smirnov, JETP Lett. **53**, 271 (1991).
24. E. Withoff, Diplomarbeit, Universität Hamburg , (1991).
25. J. B. Hastings, D. P. Siddons, L. E. Berman, and J. R. Schneider, Rev. Sci. Instrum. 60, 2398 (1989), also see P. Suortti, ESRF User's Information Meeting Proceedings, 8-9 July, 1991, Grenoble, France.

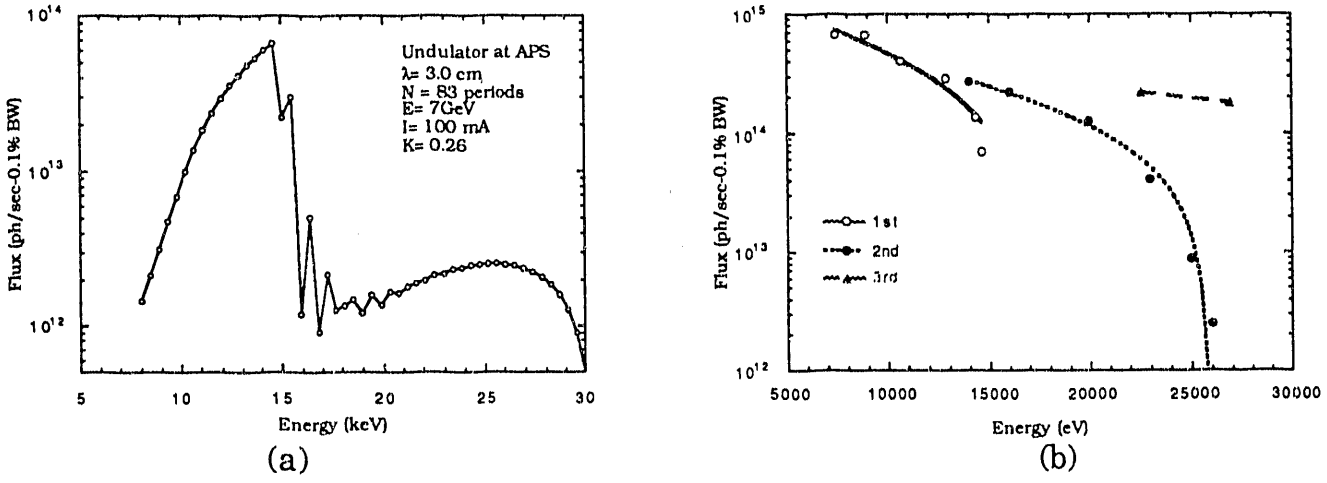

Fig. 1. (a) Calculated spectrum of radiation from an undulator source on APS, and (b) the tunability range of the first, second, and third harmonics.

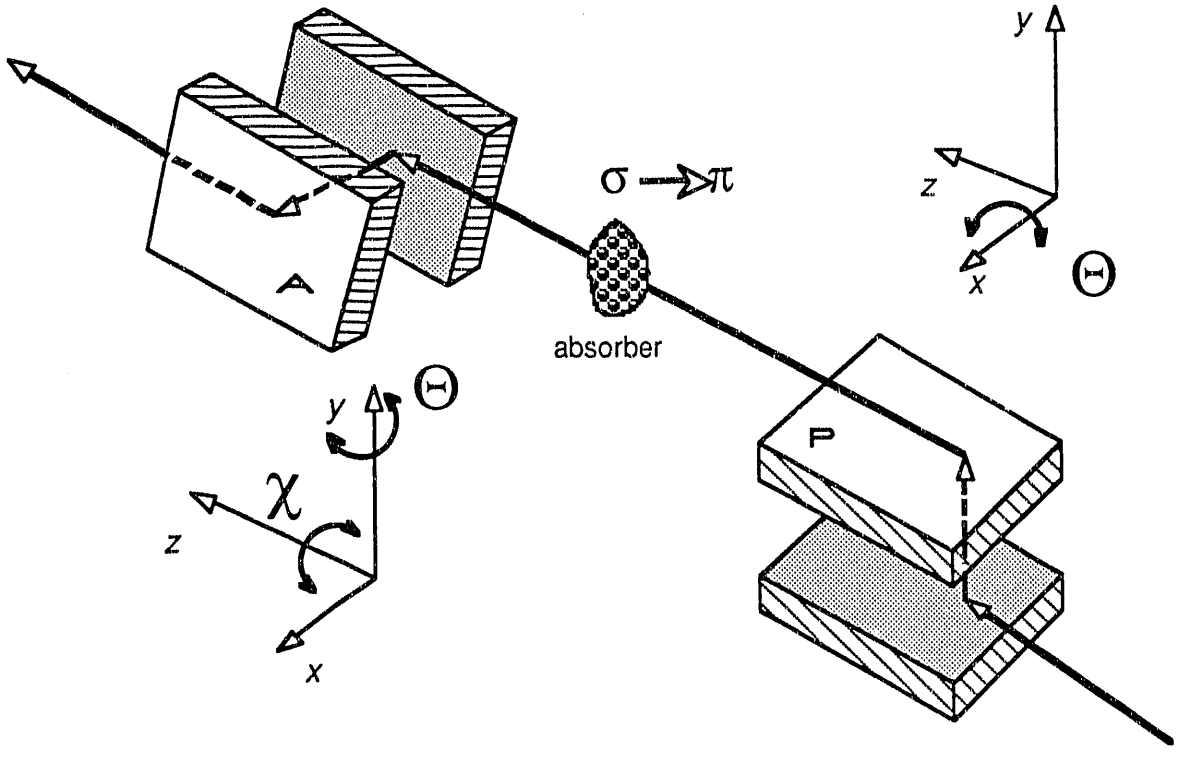

Fig. 2. Schematic arrangement of polarizing monochromator for nuclear resonant filtering. The first channel-cut crystal P acts as a polarizer, and the second channel-cut crystal A analyzes the π-component of the circularly polarized light generated as a result of nuclear absorption and emission process in the sample.

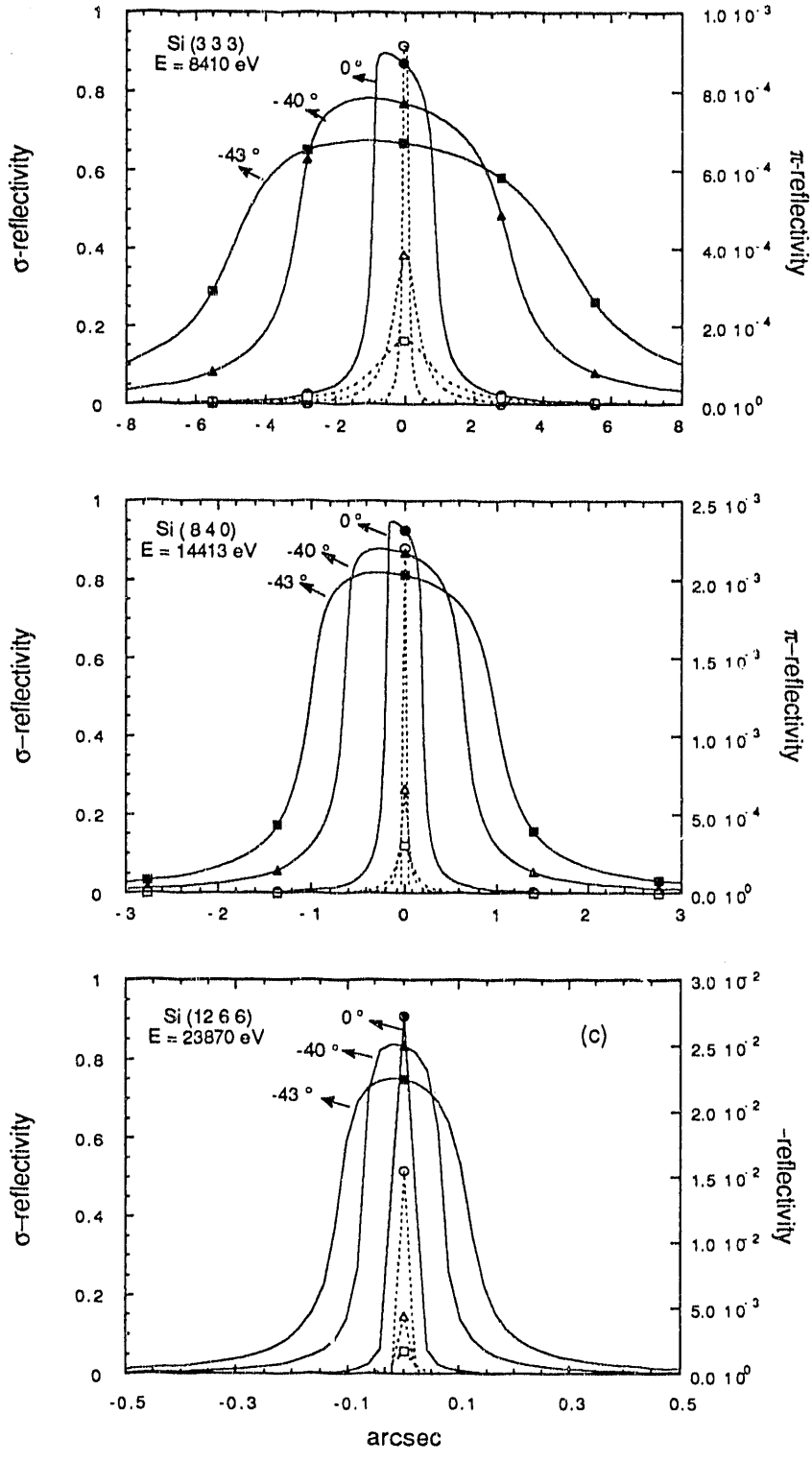

Fig. 3. The calculated reflectivity curves of (a) Si (3 3 3), (b) Si (8 4 0), and (c) Si (12 6 6) at various asymmetry angles for ^{169}Tm, ^{57}Fe, and ^{119}Sn Mossbauer resonance energies.

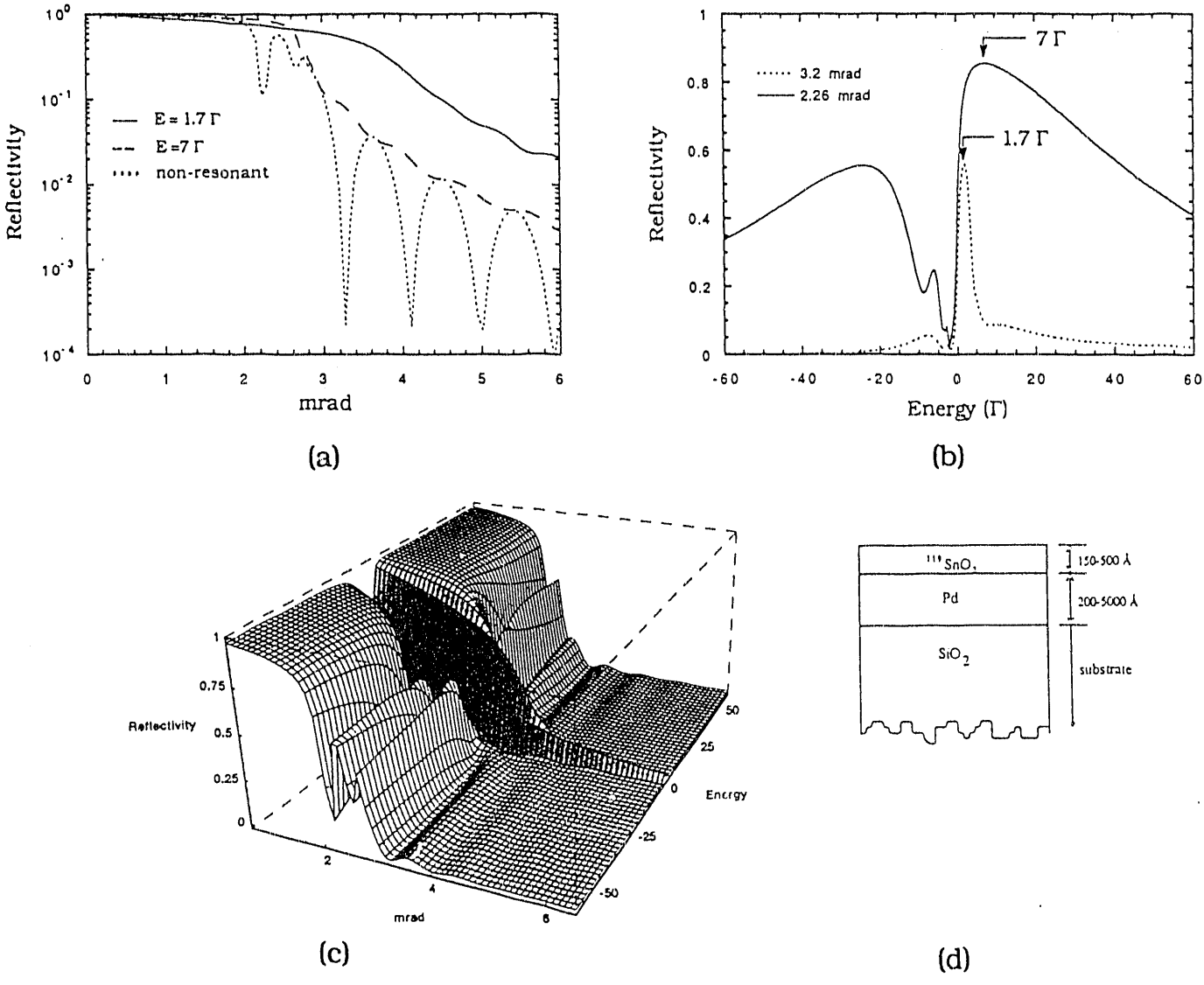

Fig. 4. (a) The calculated nuclear resonant and non-resonant reflectivity of 258 Å $^{119}SnO_2$/Pd GIAR film at 23870 eV as a function of incident angle, (b) the corresponding nuclear reflectivity as a function of deviation from resonant energy in units of linewidth, Γ, at two different incident angles, (c) three dimensional depiction of reflectivity as a function of angle and energy, and (d) schematic arrangement of the GIAR film.

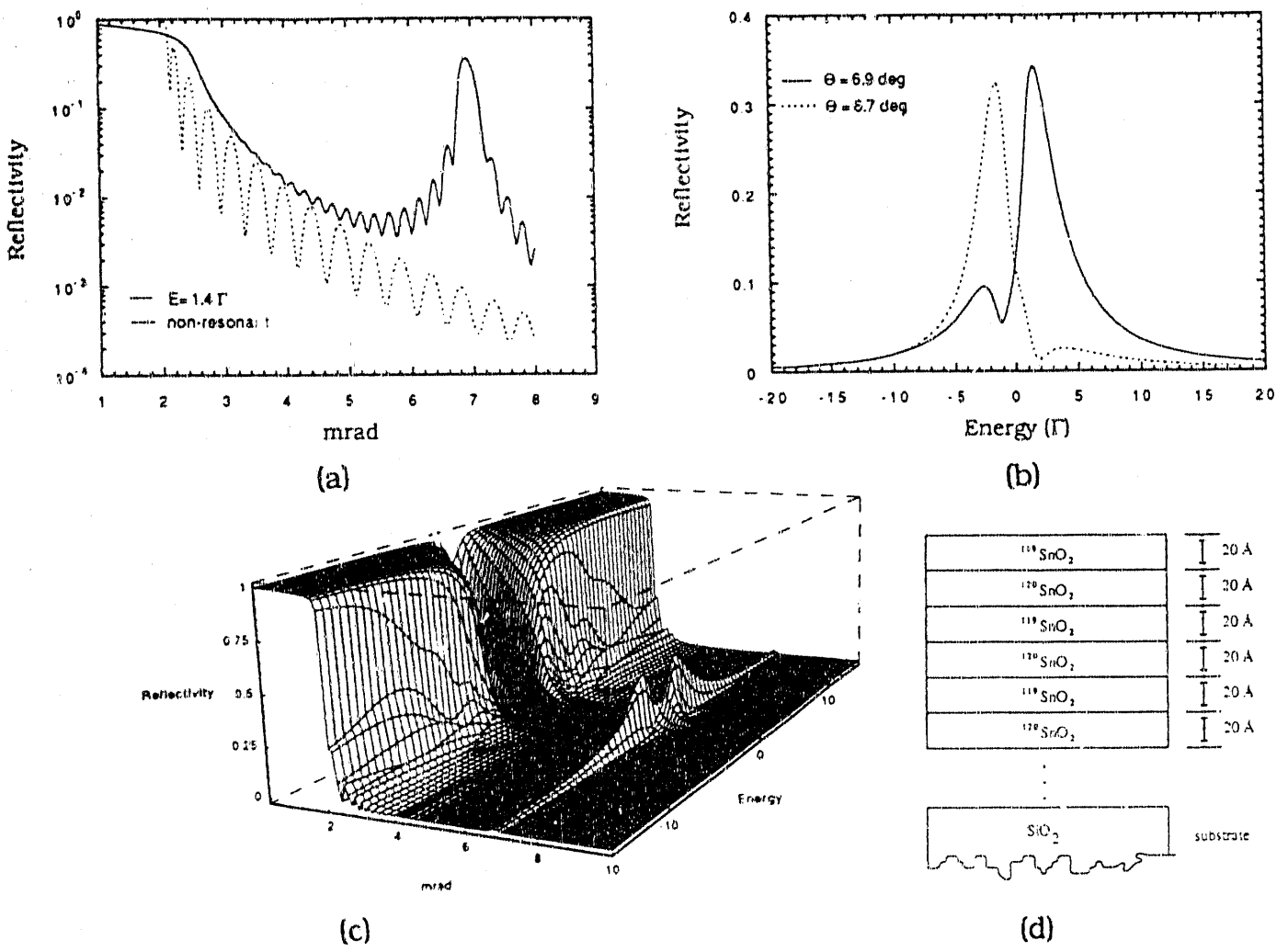

Fig. 5. (a) The calculated nuclear resonant and non-resonant reflectivity of 50 layers of 20 Å $^{119}SnO_2$ / $^{120}SnO_2$ film at 23870 eV as a function of incident angle, (b) the corresponding nuclear reflectivity as a function of deviation from resonant energy in units of linewidth, Γ, at two different incident angles (c) three dimensional depiction of reflectivity as a function of angle and energy, and (d) schematic arrangement of the multilayer monochromator.

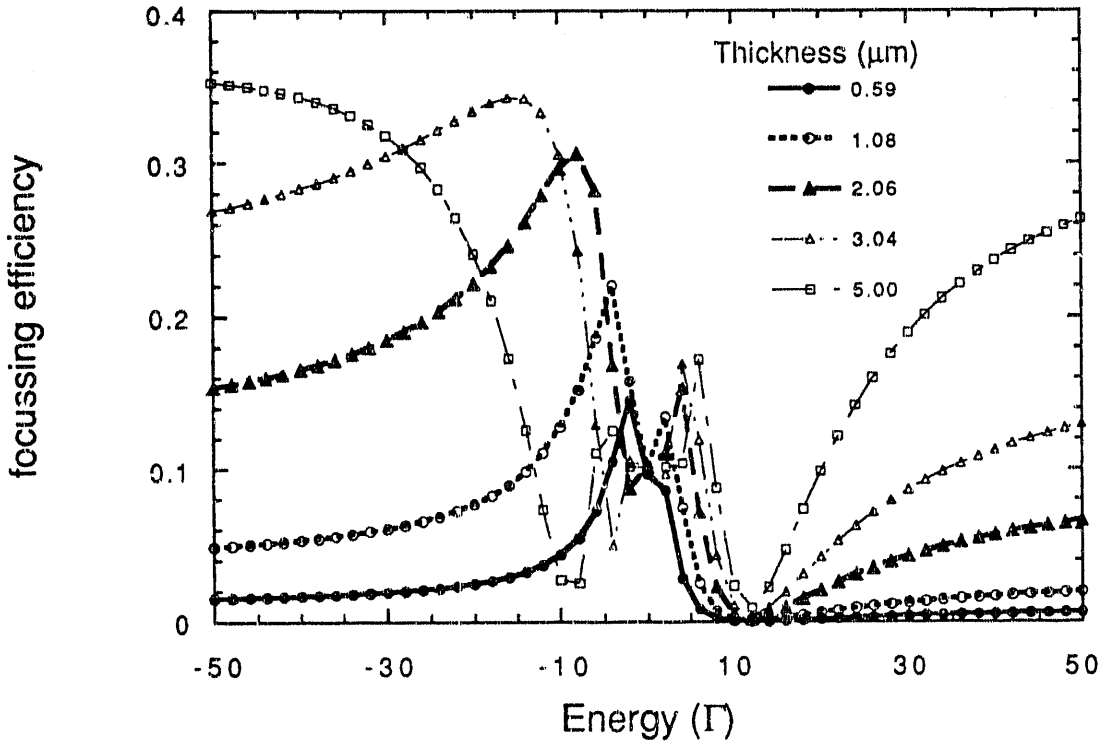

Fig. 6 . Focussing efficiency of Mossbauer-Fresenel zone plate as a function of thickness, and deviation of energy from the resonant energy for 57Fe containing zones with no internal hyperfine field.

END

DATE
FILMED
9/02/92